Comparative Photo-Oxidation under Natural and Accelerated Conditions of Polypropylene Nanocomposites Produced by Extrusion and Injection Molding

M. Diagne, M. Guèye, A. Dasilva, A. Tidjani

LRNA, Faculté des Sciences et Techniques, Université Cheikh Anta Diop de Dakar, BP 5005, Dakar-Fann, Sénégal

Received 11 October 2006; accepted 4 January 2007
DOI 10.1002/app.26459
Published online 11 June 2007 in Wiley InterScience (www.interscience.wiley.com).

ABSTRACT: The photo-oxidation behavior under natural and accelerated conditions of polypropylene/layered silicate nanocomposite is studied in this article. The nanocomposites are prepared via simple melt mixing (extrusion and injection molding). The structure obtained is very dependent on the preparation mode and the modified clay used; mostly, exfoliation structure is produced. The nanocomposites start their photo-degradation earlier than the control samples polypropylene and polypropylene-*graft*-maleic anhydride with a higher oxidation rate for specimen produced by injection molding. This is explained by the presence of organiphilic-modified montmorillonite layers that trap the oxygen, increasing the oxygen pressure in the bulk and leading to a decrease of the induction period. Contrary to the control samples that display auto acceleration in their oxidation kinetics, the nanocomposites show a slight tendency to a plateau indicating a slowing down of the photo-oxidation process. This is ascribed to oxygen starvation that occurs in the nanocomposite. The acceleration factor is found to be higher for the nanocomposite comparatively of the control samples. With the aid of SF_4 and NO treatments, the mechanism of photo degradation was found to be similar in PPgMA and its nanocomposites. © 2007 Wiley Periodicals, Inc. J Appl Polym Sci 105: 3787–3793, 2007

Key words: polypropylene-*graft*-maleic anhydride; montmorillonite; nanocomposite; photo-oxidation

INTRODUCTION

Because of their extremely high aspect ratio and to the nanometer filler thickness, clay layers were considered to be an appropriate reinforcing agent.[1] But the real story of the nanocomposites started with the discovery by Toyota scientists who discovered remarkable properties of polyamide-6 nanocomposite containing 5% clay.[2] This composite exhibited an increase in tensile, tensile modulus, flexural strength, flexural modulus, and heat distortion. From this point, attempts to produce nanocomposite with several polymers became a need that explains the numerous works available in the literature in this field today. Polymer–clay nanocomposites can be produced by three methods: intercalation of a suitable monomer followed by polymerization,[2] polymer intercalation from solution,[3] or direct melt intercalation.[4] The nanocomposites obtained are described as intercalated if the *d*-spacing between the clay platelets is maintained as the polymer inserts, exfoliated if these platelets are dispersed in the polymeric matrix, and a mixture of both.[4] Because of its huge commercial opportunities in several areas, the fabrication of Polypropylene-nanocomposite (PPCN) has become a hot area of current interest. It has been demonstrated, for PPCN containing only 5% clay, a reduction of gas permeability, an enhancement of thermal stability and fire retardancy performance as well as an improvement of mechanical properties. But one aspect that has been neglected so far is the ageing of nanocomposites; few articles are available in literature on this topic.[5–9] The common conclusion of these studies is that polymer nanocomposite photo degraded earlier than the reported host matrix. Among the explanations given, the photo degradation of the alkyl ammonium and the influence of the metallic cations are often put forward.

In numerous automotive and general/industrial applications (for example mirror housings on vehicle, door handles, timing belt covers, and so on) which demand routine exposure to solar radiation, the photochemical behavior of nanocomposites is a great challenge. It is then of interest to investigate their ageing behavior and the consequence of this degradation process on their valuable properties. For this purpose, current efforts in our laboratory focus on these aspects. Lately, a comprehensive study on the thermal stability and fire retardant performance of photo-oxidized PPCNs has been reported.[10] Here in, an extensive investigation of the photo-oxidation -under natural and accelerated conditions- of PPCN

Correspondence to: A. Tidjani (atidjani@refer.sn).

Journal of Applied Polymer Science, Vol. 105, 3787–3793 (2007)

produced by extrusion and injection molding has been conducted. Using SF_4 and NO treatments we have tried to understand the chemistry behind the photo-ageing process.

EXPERIMENTAL

Materials

The materials used for the production of PP nanocomposite are commercial products. Polypropylene graft maleic anhydride (from Aldrich, containing 0.6% of maleic anhydride) was blended with three different commercial organiphilic-modified montmorillonites (OMMT). The first two, Cloisite 30B and Cloisite 20A from Southern Clays Products, were modified with a quaternary ammonium salt methyl tallow bis2hydroxethyl (MT2EtOH) and dimethyl dihydrogenatedtallow (2M2HT), respectively. The third is a product from Nanocor named Nanomer I28E, ion exchanged with an octadecyl trimethyl amine (OD3MA).

Preparation of the nanocomposites

A first series of PPCN was produced by extrusion using an intermeshing twin-screw extruder Haake Rheomex TW 100. The ingredients were mixed simultaneously without any processing stabilizer at a screw speed of 50 rpm at 458 K. Films (150–300 μm) were obtained by pressing the resulting material with a hydraulic press. For comparison, a second series of specimen was produced by extrusion followed by injection molding using a ZSK 25 machine (Werner und Pfeider, Germany) through nine temperature zones going from 448 to 462 K; injection molding operation was carried out at 453 K under a pressure of 900 bar and a post pressure of 350 bar for 4 s. In all cases, the final films of PPCN formulations are 5% organoclay/95% PPgMA by weight %.

Instrumentation

Evaluation of microstructure

The nanocomposites were characterized in terms of their nanoscale arrangement using a combination of X-ray diffraction, XRD, and transmission electronic microscope (TEM). Details on these techniques can be found in a previous article.[10]

UV irradiation conditions

The accelerated weathering tests were performed in a SEPAP 12-24 unit at a working temperature of 60°C. In this apparatus, which has been extensively described elsewhere,[11] the incident polychromatic beam was filtered using appropriate cut-off filters to eliminate the radiation of wave lengths shorter than 300 nm. The main reason for this elimination was their irrelevance to natural photo-ageing. Nowadays, there is a need to validate the photo-ageing results obtained at the laboratory level through ageing under natural conditions. Taking advantage of the tropical climate in Dakar, Senegal, located at 17°E longitude and 15°N latitude, photo-ageing under natural conditions was conducted on films mounted on wooden racks inclined at 15° to the horizontal.[12]

Analytical measurement

The chemical changes occurring in the films after UV irradiation were followed by FTIR technique. A Perkin–Elmer BX II, at a 4 cm^{-1} resolution, was used to collect the FTIR spectra. To further characterize and quantify the results of the oxidation process, photo-oxidized samples have been treated with SF_4 and NO.[13,14] The SF_4 treatment allows an exact quantification of carboxylic acids then a deduction of ketone and ester species concentration. The determination of alcohol and hydroperoxide concentrations and their structures (primary, secondary, and tertiary state) is possible with the NO treatment.

RESULTS AND DISCUSSION

Characterization of nanocomposites

Figure 1 displays the X-ray diffraction patterns of modified montmorillonite and their corresponding nanocomposites produced by extrusion or by injection molding. It can be observed for PPgMA-2M2HT nanocomposites that the d_{001} peak was broadened with low intensity and shift towards lower angles whatever the mode of production. The broadening of the peak makes difficult to evaluate the intergallery spacing; however, the shift to lower angle is unquestionable. The TEM micrographs of PPgMA-2M2HT presented in Figures 2 and 3 suggested that a good dispersion and a mixed intercalated-exfoliated system were obtained using extrusion and injection molding mode of preparation, respectively.

In the case of PPgMA-MT2EtOH nanocomposite, influence of the mode of preparation is clearly evidenced by the results displayed. For specimen prepared by injection molding, a similar situation that was described for PPgMA-2M2HT is noticed. As for the extruded blending PPgMA-MT2EtOH sample, a decrease of the *d*-spacing is observed. The structure of this sample revealed by the TEM images was closed to a tactoid structure.

The third type of nanocomposites -prepared with OD3MA- was totally exfoliated in the injection molding mode and, intermediate between an exfoliated

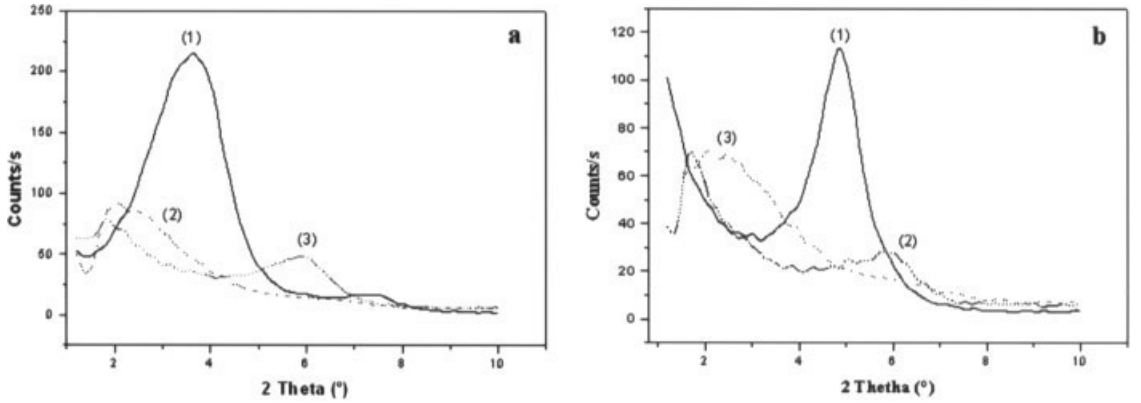

Figure 1 X-ray diffraction patterns of Cloisite 20A-2M2HT—(Fig. a, curve 1) and Cloisite 30 B -MT2EtOH—(Fig. b, curve 1) and their nanocomposites produced by extrusion (curve 2) or by injection molding (curve 3).

and tactoid state in the extrusion mode. All these results collected in this part are summarized in Table I. Here in, it is worth mentioning that the dependence on the type of modified clay used is more clearly seen on extruded blending PP-nanocomposites; this stresses the importance of the preparation mode on the production of true nanocomposites. Besides the effect of the production mode, the effect of silicate functionalization and intermolecular interactions on the final structure could be of importance. So far, these parameters are not well understood.

Photo-oxidation of nanocomposites

Oxidation of the exposed nanocomposites was followed through the irradiation process using FTIR technique. The evolution of the infrared spectrum, in the carbonyl region upon UV irradiation, reveals first a decrease of the 1780 cm^{-1} band corresponding to the disappearance of maleic anhydride. In the following, we observe the formation of ketones and carboxylic acids that absorb around 1715 cm^{-1}, ester and γ-lactone species that absorb at 1740 and 1780 cm^{-1}, respectively. An unexpected band centered at 1564 cm^{-1} appears and increases with UV irradiation time; this band—which was not an artifact—appeared in all nanocomposites and PPgMA but not in pure PP. For analysis of the detailed photo-degradation process, one other domain of the infrared spectrum may be of interest, i.e., the hydroxyl region. In this region, a broad band centered at 3400 cm^{-1} increases regularly upon UV irradiation. This band is ascribed to the O—H stretching of hydroperoxyde and alcohol groups.

Comparing these observations to those noticed during the photo-oxidation of pure PP, besides intensities of the bands, the main difference comes from the band at 1564 cm^{-1} in the present spectra. This band has been ascribed to salt band in different experimental conditions.[15] In our case, this band could be attributed to ionized acid. This speculation is substantiated by the fact that during the SF_4 treat-

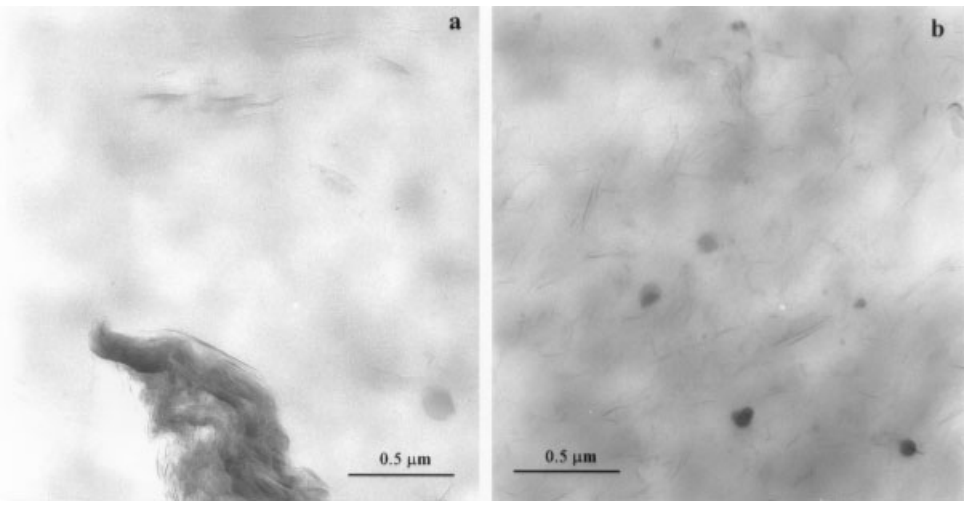

Figure 2 TEM images of PP-MT2EtOH (a) and PP-2M2HT (b) nanocomposites produced by extrusion.

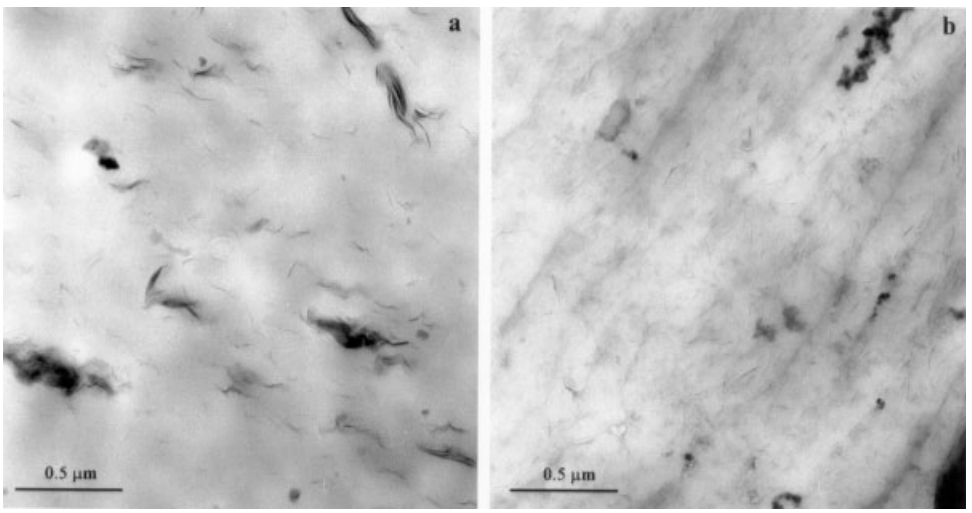

Figure 3 TEM images of PP-2M2HT (a) and PP-MT2EtOH (b) prepared by injection molding.

ment, we notice the disappearance of this band balanced by the appearance of a new band between 740 and 750 cm^{-1}.

Influence of the preparation mode of nanocomposite on the photo degradation

Figure 4 shows the infrared absorbance—in the carbonyl region—of nanocomposites produced by injection molding and extrusion and photo degraded to approximately the same level of oxidation.

Comparison of the shapes of the IR spectra obtained shows an apparent effect of the production mode of nanocomposite on the photo degradation process. Absorbance of the bands at 1780 cm^{-1} (γ-lactones) and 1735–1740 cm^{-1} (esters) are slightly higher for samples prepared by injection molding than those produced by extrusion under both UV irradiation conditions. This observation is more obvious under accelerated conditions than under natural ones. The oxidation kinetics depicted in Figure 5 reveal that samples prepared by injection molding oxidize faster that those produced by extrusion, whatever the experimental conditions. On the other hand, the nanocomposites prepared by extrusion displayed a higher absorbance at 1564 cm^{-1} in comparison to samples produced by injection molding.

From these results, it seems that specimens produced by injection molding are more keen to photo-oxidation than those prepared by extrusion. This difference could be ascribed to the state of mixing of the nanocomposite produced. Indeed, it was previously observed that the level of exfoliation was much better in injection molded samples than in extruded samples. This get the support to the fact that the degrading effect plays by the nanofiller increases with the dispersion of the clay platelets within the polymeric matrix.[8]

It can be also observed in Figure 5 that the nanocomposites show higher propensity to photo oxidation than the control samples (PPgMA and PP). This indicates that the presence of OMMT in PP matrix exacerbates the photo-oxidation, as evidenced by a reduction of the induction period of nanocomposites comparatively to PP and PPgMA. On the other hand, the accumulation kinetics of carbonyl species for the nanocomposites shows a slight tendency to a plateau. The ultimate consequence is that the control samples display a higher level of degradation than the nanocomposites. For example, after 4000 h of natural exposure, the normalized absorbance at 1715 cm^{-1} of PP is 1.4 compared to an average of 0.5 for most nanocomposites. These results can be explained by the fact that the presence of OMMT may play a twin role during the degradation process. Before any UV irradiation, oxygen—that may be able to diffuse in the bulk of the nanocomposite—is trapped due to the presence of silicate layers.

TABLE I
XRD and TEM Results of the Polypropylene-Nanocomposites Produced by Extrusion and Injection Molding

Mode of preparation	Characterization technique	PPgMA-2M2HT	PPgMA-MT2EtOH	PPgMA-OD3MA
Extrusion	XRD	Diffuse peak	Decrease of d-spacing	Diffuse peak
	TEM	Good exfoliation	Tactoid	Tactoid-exfoliation
Injection molding	XRD	Diffuse peak	No peak	Diffuse peak
	TEM	Very good exfoliation	Best exfoliation	Exfoliation

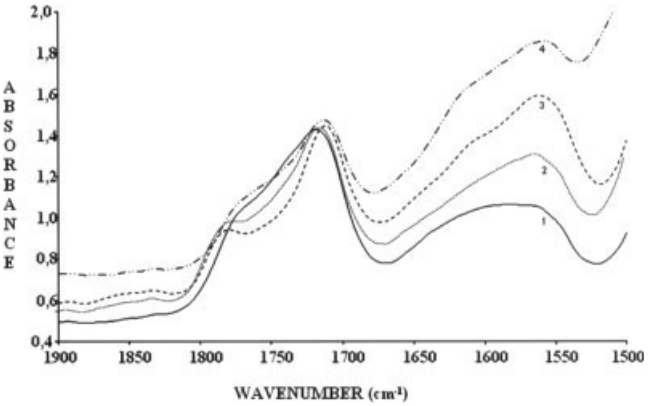

Figure 4 FTIR spectra of PPgMA-2MT2HT nanocomposite blended by injection molding and exposed under accelerated (1) and natural (4) conditions; spectra labelled (2) and (3) corresponds to PPgMA-2MT2HT blended by extrusion and exposed under accelerated and natural conditions, respectively.

This phenomenon may induce an increase in oxygen pressure in the bulk. According to the Verdu group, an oxygen pressure increase leads to a decrease in the induction time;[16] this is evidenced by the earlier photo degradation of the nanocomposites comparatively to the control samples. But once the oxygen trapped is consumed at the beginning of the oxidation process, starvation of oxygen may occur due to a difficulty of the gas to permeate in the nanocomposite because of the clay platelets presence.[17] This starvation of oxygen induces a reduction of the degradation of nanocomposites leading to the pseudo-plateau noticed in the kinetic accumulation of carbonyl groups.

Another phenomenon that can contribute to the reduction of the induction time could be the presence in the organoclays of trace amount of metal ions that may promote catalytic photo degradation.[9]

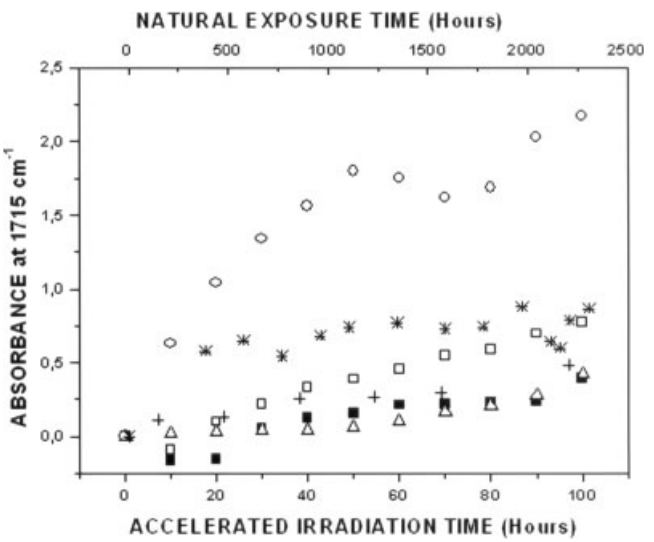

Figure 5 Variation of the carbonyl band (normalized at 100 μm) during the photo-oxidation under accelerated conditions of PP (Δ), PPgMA (■), PPgMA-2MT2HT blended by extrusion (□) and by injection molding (o); the remaining symbols (+, *) stand respectively, for PPgMA-2MT2HT blended by extrusion and by injection molding and, natural UV irradiated.

Influence of mode of UV irradiation on the photo degradation/acceleration factor

It is of interest to notice on Figure 5 a negative variation of the absorbance at 1715 cm^{-1} of nanocomposite and PPgMA at the very beginning of accelerated photo ageing. This is an evidence of the decomposition of maleic anhydride at the beginning of UV exposure; this decomposition may yield to the formation of oxidation products according to the following reaction:

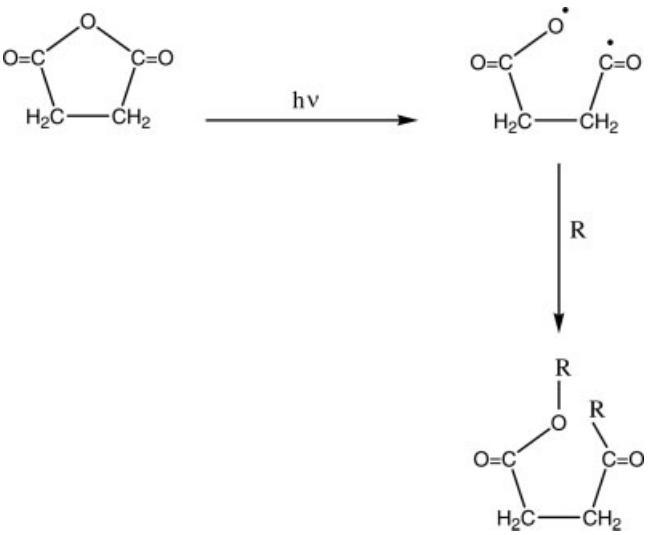

where R could be H, OH or a radical.

In opposite, under natural irradiation, this decomposition is no longer observed as shown in Figure 5. This indicates a stoichiometry difference between the two modes of UV irradiation. The flux of photons, the working temperature, and the diffusion of oxygen could be the major causes of such discrepancies. However, this stoichiometry difference is not apparent by comparing the shapes of the curves of the two series of specimen obtained under both modes of UV irradiation.

TABLE II
Acceleration Factor Calculated at 0.1 Absorbance at 1715 cm^{-1}

Sample	Extrusion	Injection molding
PP	19.70	19.62
PPgMA	18.46	20.62
PPgMA-OD3MA	40.08	39.54
PPgMA-2M2HT	37.94	36.31
PPgMA-MT2EtOH	22.90	21.81

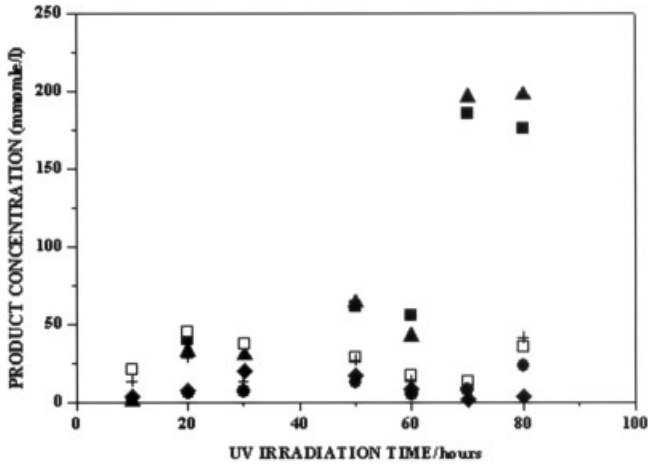

Figure 6 Evolution of the oxidation products versus the UV irradiation time during accelerated test of the control sample PPgMA: (▲) ester, (■) ketone, (□) tertiary hydroperoxide, (+) secondary hydroperoxide, (●) alcohol, (◆) acid.

One of the objectives of running natural and accelerated tests is to determine the acceleration factor to accurately predict the life service of polymers in use. So far, the determination of this acceleration factor is done by trial and error and, remains difficult and not entirely satisfactory. A scientific criteria based on carbonyl growth can be used. The acceleration factor is then defined as the ratio between the times estimated under natural and accelerated photo ageing to reach 0.1 absorbance at 1715 cm^{-1}. The obtained data are presented in Table II.

Whatever the preparation mode of nanocomposite, the acceleration factor of the two nanocomposites PPgMA-2M2HT and PPgMA-OD3MA increases significantly comparatively to the control samples. This increase can be explained by the oxygen starvation mentioned previously. By slowing down the degradation kinetics, this phenomenon augments the acceleration factor. It is worth mentioning that no effect of the mode of nanocomposite production is noticed. For PPgMA-MT2EtOH, the situation is tricky because MT2EtOH is much more sensitive to degradation than the other modified clays used,[18] which explain the relative low acceleration factor of its nanocomposites.

Accumulation kinetics of oxidation products

Figures 6 and 7 exhibit the kinetic curves of quantified oxidation photoproducts. This quantification was done using SF_4 and NO treatments. For the control sample (Fig. 6), a short induction period is observed for some species (ester and ketone). An auto-acceleration is subsequently noticed for the generation of ester and ketone, which are the dominant photoproducts. No significant variation in their formation is displayed for the other photoproducts. It should be reminded that during the photo oxidation of pure PP, ketone groups appear to be the dominant photoproducts followed by acid and ester groups, which are produced to roughly the same extent.[12] An example of kinetic accumulation of oxidation products of a nanocomposite is depicted in Figure 7. The kinetic curve displays an auto-accelerated shape without any induction period for most photo-products, confirming the rapid initiation of degradation in the nanocomposites. Ketone and ester groups are still the dominant products followed by hydroperoxide and alcohol entities. The major remarks from the comparison of kinetic accumulation of oxidation products in PPgMA, nanocomposite and pure PP are: (i) a very low concentration of acid groups is noticeable in PPgMA and nanocomposites comparatively to pure PP and (ii) favorable production of ester and ketone species at the expense of other oxidation products is observed in PPgMA and somehow in nanocomposites. It is worth mentioning that stoichiometry changes underscored previously for both types of nanocomposites are not visible in the quantification of the oxidation products. These results give an indication that the reactions involved in the photo degradation process of PPgMA and its nanocomposites are not much different. Using the changes in mechanical properties and chemical structure, other authors got to the same conclusion.[8,9] On the other hand, the pathway of degradation of PPgMA and its nanocomposites displayed some differences with the one of pure PP; the striking observation was the low generation of acid species in the first ones. According to the literature, carboxylic acids may originate from ketone,

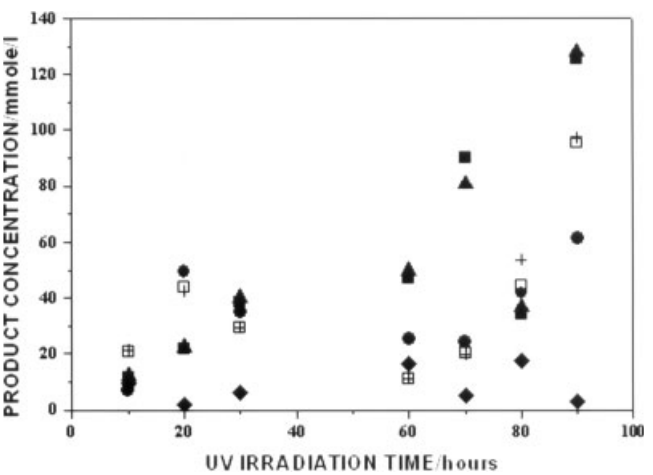

Figure 7 Evolution of the oxidation products versus the UV irradiation time during accelerated test of PPgMA-2M2HT: (▲) ester, (■) ketone, (□) tertiary hydroperoxide, (+) secondary hydroperoxide, (●) alcohol, (◆) acid.

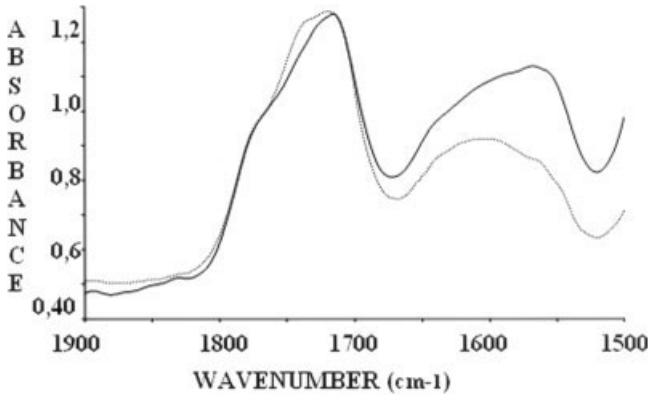

Figure 8 FT-IR spectra in the carbonyl region of PPgMA (dashed line) and PPgMA-OD3MA (solid line) taken at the same level of oxidation from the measurement of the absorbance at 1715 cm^{-1}.

per-acid, aldehyde, hydroperoxide decomposition, and/or by radicalar reaction. Our results indicate that none of these reactions seems to be favorable in our experimental conditions.

On the other hand, formation of carboxylic acid salt was observed, may be at the expense of carboxylic acid. In Figure 8, the IR spectra in the carbonyl region of PPgMA and PPgMA-OD3MA nanocomposite taken at the same level of oxidation were displayed.

One can observe a much higher absorbance of the carboxylic acid salt band in the nanocomposite than in pure PPgMA. In this last specimen, the band at 1564 cm^{-1} was mainly ascribed to carboxylate issue from reaction between carboxylic acid and water. On the other hand, additional carboxylic acid salt due to the presence of ammonium ions could absorb at this wavenumber in the nanocomposite, which explains the difference noticed in Figure 8.

CONCLUSIONS

PPgMA/layered silicate nanocomposites were prepared using two different techniques: extrusion and injection molding. The structure obtained is very dependent on the preparation mode and the modified clay used; mostly, exfoliation structure is produced. The true nanocomposites show a higher propensity to photo-oxidation than the control samples under both natural and accelerated conditions. This is explained by the presence of OMMT layers that trap the oxygen, increasing the oxygen pressure in the bulk and leading to a decrease of the induction period. This reduction of the induction period may also originate from the presence of metal ions that promote catalytic photo degradation.[9] Contrary to the auto acceleration observed in the kinetic accumulation of carbonyl species in PPgMA and PP, the nanocomposites show a slight tendency to a plateau with a higher oxidation rate for samples produced by injection than those processed by extrusion. This phenomenon is ascribed to the starvation of oxygen that may occur in the nanocomposites due to the difficulty for the gas to permeate because of the presence of the clay platelets. The direct consequence is the significant increase of the acceleration factor of the nanocomposites compared to the ones calculated for the control samples. An unexpected band absorbing at 1564 cm^{-1} appeared during the photo-degradation of the nanocomposite and PPgMA; it is tentatively attributed to carboxylic acid salt with the aid of SF_4 treatment.

The quantification of oxidations products with SF_4 and NO treatments highlights the predominance of ester and ketone species and a surprising low concentration of acid groups in nanocomposites and PPgMA. If the chemical pathway of degradation is similar in PPgMA and its nanocomposites, it is different to what was observed in pure PP.

References

1. Shepherd, P. D.; Golemba, F. J.; Maine, F. W. Adv Chem Ser 1974, 134, 41.
2. Kojima, Y.; Usuki, A.; Kawasumi, M.; Okada, A.; Fukushima, Y.; Kurauchi, T.; Kamigaito, O. J Mater Res 1993, 8, 1185.
3. Lan, T.; Pinnavia, T. Chem Mater 1994, 6, 2216.
4. Porter, D.; Metcalfe, E.; Thomas, J. K. Fire Mater 2000, 24, 45.
5. Tidjani, A.; Wilkie, C. A. Polym Degrad Stab 2001, 74, 33.
6. Mailhot, B.; Morlat, S.; Gardette, J. L.; Boucard, S.; Duchet, J.; Gérard, J. F. Polym Degrad Stab 2003, 82, 163.
7. Qin, H.; Zhang, S.; Liu, H.; Xie, S.; Yang, M.; Shen, D. Polymer 2005, 46, 3149.
8. Morlat-Therias, S.; Fanton, E.; Tomer, N. S.; Rana, S.; Singh, R. P.; Gardette, J. L. Polym Degrad Stab 2006, 91, 3033.
9. La Mantia, F. P.; Tzankova Dintcheva, N.; Malatesta, V.; Pagani, F. Polym Degrad Stab 2006, 91, 3208.
10. Diagne, M.; Guèye, M.; Vidal, L.; Tidjani, A. Polym Degrad Stab 2005, 89, 418.
11. Pernot, G.; Arnaud, R.; Lemaire J Die Ang. Makromol Chem 1983, 117, 71.
12. Tidjani, A.; Arnaud, R. Polym Degrad Stab 1993, 39, 285.
13. Carlsson, D. J.; Brousseau, R.; Zhang, C.; Wiles, D. M. ACS Symposium Series 364, September 7–12 1986; p 376.
14. Tidjani A. J Appl Polym Sci 1997, 64, 2497.
15. Sclavons, M.; Franquinet, P.; Carlier, V.; Verfaillie, G.; Fallais, I.; Legras, R.; Laurent, M.; Thyrion F C. Polymer 2000, 41, 1989.
16. Richaud, E.; Farcas, F.; Bartoloméo, P.; Fayolle, B.; Audouin, L.; Verdu, J. Polym Degrad Stab 2006, 91, 398.
17. Tidjani, A. Polym Degrad Stab 2005, 87, 43.
18. Tidjani, A.; Wald, O.; Pohl, M. M.; Hentschel, M. P.; Schartel, B. Polym Degrad Stab 2003, 82, 133.